

## Supporting Information

### **Novel Surfactant-directed Synthesis of Ultrathin Palladium Nanosheets as Efficient Electrocatalyst for Glycerol Oxidation**

*Dongdong Xu\**, *Ying Liu*, *Shulin Zhao*, *Yanan Lu*, *Min Han*, *Jianchun Bao\**

*Jiangsu Collaborative Innovation Center of Biomedical Functional Materials, School of Chemistry and Materials Science, Nanjing Normal University, Nanjing, 210023, P. R. China*

#### **Experimental Sections**

##### **Chemicals and materials.**

Commercial palladium (II) chloride (99.9 wt%), L-ascorbic acid (99%) and palladium black were purchased from Alfa Aesar. Hydrochloric acid, pyridine, hydrazine hydrate, sodium borohydride, ethanol, acetonitrile, and diethyl ether were obtained from Sinopharm Chemical Reagent Co. Ltd. (Shanghai). 1-Bromodocosane (98%), 1-Bromoeicosane (95%), 1-Bromooctadecane (97%), 1-Bromohexadecane (96%), and 1-Bromotetradecane (97%) were purchased from TCI corporation. H<sub>2</sub>PdCl<sub>4</sub> solution (10 mM) was prepared by dissolving 0.3550 g palladium (II) chloride in HCl solution (20 mL, 0.2 M) and further diluting to 200 mL with deionized water. All the reagents were of analytical reagent grade and used without further purification.

##### **Synthesis of pyridinium-type surfactants.**

Take the preparation of C22-pyB for an example, 3.9 g of 1-Bromodocosane (10 mmol) and 1.2 g (15 mmol) of pyridine were mixed in 200 ml of acetonitrile and refluxed under 368 K for 20 hours. After cooling to room temperature, the solvent was removed by reduced pressure distillation. Then, the crude product was washed with diethyl ether and dried in a vacuum oven overnight. The pyridinium-type surfactants with different alkyl chain length (C20-pyB, C18-pyB, C16-pyB and C14-pyB, see Fig. S1) were also obtained following the similar procedures by substituting 1-Bromodocosane with 1-Bromoeicosane, 1-Bromooctadecane, 1-Bromohexadecane, and 1-Bromotetradecane, respectively. All of products were verified by <sup>1</sup>H NMR. Here, take the surfactant C22-pyB for an example (Fig. S2): <sup>1</sup>H NMR (400 MHz, CD<sub>3</sub>OD): δ 9.04 (d, J = 5.7 Hz, 2H), 8.67-8.58 (m, 1H), 8.14-8.10 (t, J = 7.0 Hz, 2H), 4.66-4.62 (m, 2H), 1.51-1.19 (m, 40H), 0.92 (t, J = 6.9 Hz, 3H).

Docosylpyridinium chloride (C22-pyC) and Docosylpyridinium iodide (C22-pyI) were prepared as follows: C22-pyB was converted to hydroxide-type C22-py(OH) by passing aqueous solution through a column packed with anion exchange resin. Then, C22-py(OH) was neutralized by a little excess HCl and HI solution, respectively. Solid C22-pyC and C22-pyI were obtained through the removal of water in a vacuum-freezing drier.

#### **Synthesis of ultrathin Pd nanosheets.**

In a typical synthesis of ultrathin Pd nanosheets, 0.094 g C22-pyB was dissolved in 10 mL deionized water, and then 3.0 ml H<sub>2</sub>PdCl<sub>4</sub> solution (10 mM) was added. After homogeneous mixing, a freshly prepared L-ascorbic acid (AA, 0.5 M, 1.0 mL) was rapidly injected into the above solution. The aging process was kept under 35 °C or room temperature. The color of the reaction solution slowly changed from brownish yellow to black in the following several hours. After the complete reduction of Pd precursor, ultrathin Pd nanosheets were collected by centrifugation and washed with ethanol several times. The as-made PdNSs were also illuminated by a UV/ozone cleaning instrument (100 W, with 185 nm and 254 nm emissions) at the distance of about 5 mm for 2 hours to remove the residual organic surfactants before characterization and electrochemical measurements. The other Pd nanostructures synthesized by different surfactants or under distinct temperature and concentration were operated following the similar process.

#### **Characterization.**

The transmission electron microscope (TEM) observation was performed with a JEOL JEM-2100 microscope operated at 200 kV (Cs 1.0 mm, point resolution 2.3 Å). Images were recorded with a KeenView CCD camera (resolution 1376 x 1032 pixels, pixel size 6.45 x 6.45 μm). X-ray diffraction patterns were recorded on a powder sample using a D/max 2500 VL/PC diffractometer (Japan) equipped with graphite-monochromatized Cu Kα radiation in 2θ ranging from 1° to 90°. Related work voltage and current were 40 kV and 100 mA, respectively. The ultrahigh resolution thermal-field emission scanning electron microscope (FE-SEM) images were obtained on a JSM-7600F apparatus at an accelerating voltage of 10 kV. <sup>1</sup>H NMR spectra were recorded on Avance III HD 400 spectrometer (400MHz), and the chemical shifts are reported in ppm relative to the residual deuterated solvent and the internal standard tetramethylsilane. The atomic force microscope (AFM) studies were performed by means of a Nanoscope IIIa scanning probe microscope (Agilent, USA) under tapping mode.

### **Electrochemical measurements.**

The electrocatalytic tests were carried out on the CHI 660E electrochemical analyzer at room temperature. A standard three-electrodes system was employed for all electrochemical tests in this work, which consisted of a platinum slice as the counter electrode, a KCl-saturated silver/silver chloride electrode (SSE) as the reference electrode, and a catalyst coated glassy carbon electrode (GCE,  $0.07065 \text{ cm}^2$ ) as the working electrode. All of potentials in this study were reported with respect to the SSE.

A well dispersed suspension of Pd catalyst was prepared by mixing 2 mg Pd nanoparticle and 1 mL ethanol and  $\text{H}_2\text{O}$  (volume ratio of 1:3) under ultrasonic for 20 min. Then, 40  $\mu\text{L}$  of 5.0 wt % Nafion solution was added and the obtained solution was allowed under ultrasonic for another 10 min. A total of 5  $\mu\text{L}$  such catalyst ink was coated on pre-treated GCE using a microliter syringe. The catalyst coated GCE was thoroughly dried in  $50^\circ\text{C}$ . Electrochemical measurements were performed in a  $0.5 \text{ mol L}^{-1}$   $\text{N}_2$ -saturated  $\text{H}_2\text{SO}_4$  solution and  $0.1 \text{ mol L}^{-1}$  glycerol +  $1 \text{ mol L}^{-1}$  KOH. In the CV measurements in  $\text{H}_2\text{SO}_4$  solution, the electrode potential was scanned in the range of  $-0.2$ - $1.0 \text{ V}$  versus Ag/AgCl at a scan rate of  $50 \text{ mV}\cdot\text{s}^{-1}$ . In the CV measurements in glycerol + KOH, the electrode potential was scanned in the range of  $-0.8$ - $0.4 \text{ V}$  versus Ag/AgCl at a scan rate of 10, 30, 50, 70, and  $100 \text{ mV}\cdot\text{s}^{-1}$ , respectively.

The electrochemically active surface areas (ECSA) of Pd catalysts were calculated from the following equation by Woods <sup>[1]</sup>:

$$\text{ECSA} = Q / (m \cdot C)$$

where  $m$  was the loading amount of Pd metal. The ECSA was calculated by integrating the reduction charge ( $Q$ ) of surface  $\text{Pd}(\text{OH})_2$  monolayer and assuming a value of  $420 \mu\text{C}\cdot\text{cm}^{-2}$  ( $C$ ).

Chronoamperometry curves were obtained in an  $\text{N}_2$ -saturated  $0.1 \text{ mol L}^{-1}$  glycerol and  $1 \text{ mol L}^{-1}$  KOH solution for 8000 s at  $-0.2 \text{ V}$  applied potential.

For the CO stripping voltammetry measurements, CO gas was bubbled through a  $0.1 \text{ mol L}^{-1}$   $\text{H}_2\text{SO}_4$  solution for 20 minutes with the presence of the electrode. After the Pd catalyst (on the surface of electrode) was fully adsorbed by CO molecules, the electrode was quickly moved to a fresh  $0.1 \text{ mol L}^{-1}$   $\text{H}_2\text{SO}_4$  solution and the CO stripping voltammetry was recorded at a scan rate of  $2 \text{ mV/s}$ .

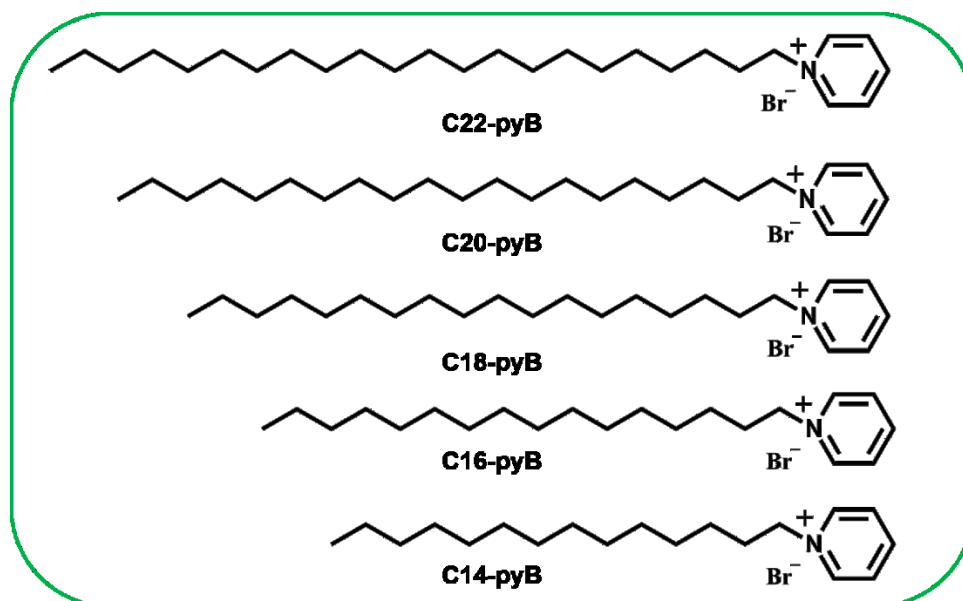


**Figure. S1.** Molecular structure of the pyridinium-type surfactants used in this work.

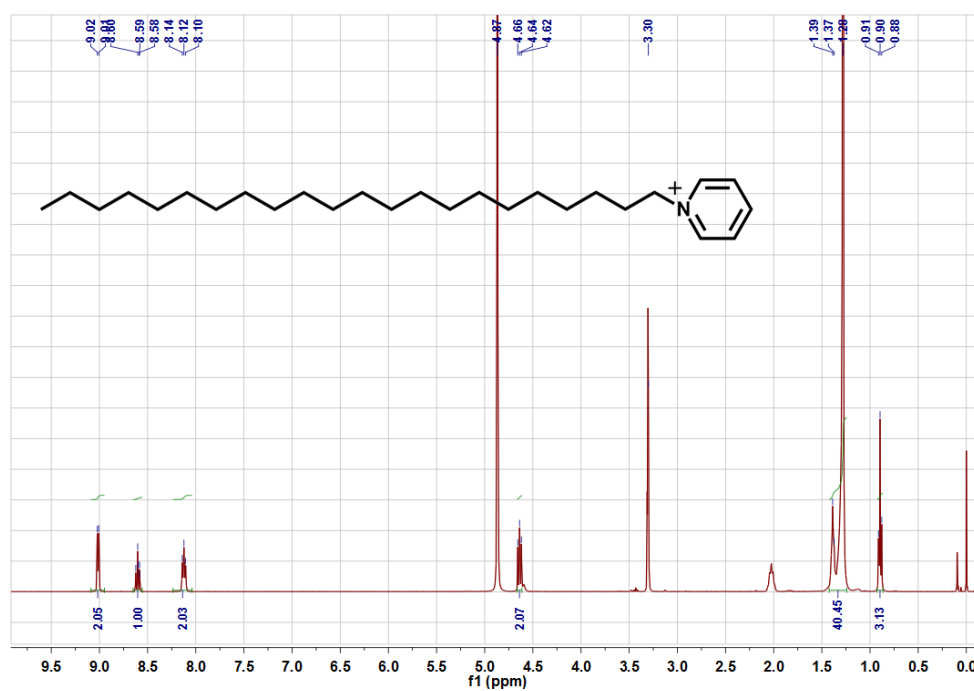


**Figure. S2.**  $^1\text{H}$  NMR spectra ( $\text{CD}_3\text{OD}$ ) of surfactant C22-pyB.

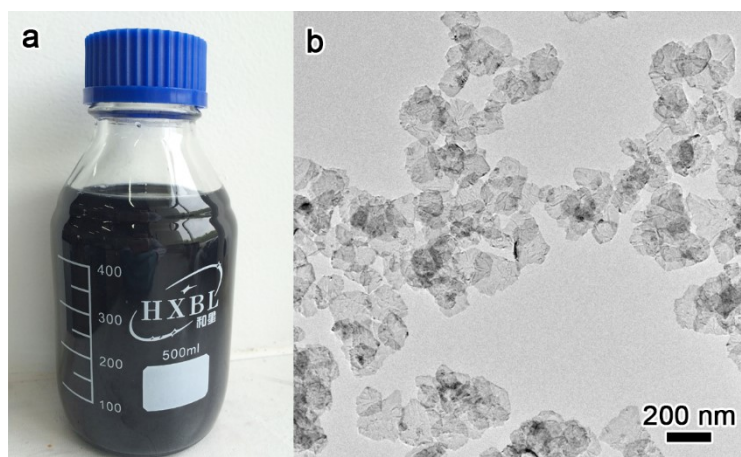


**Figure. S3.** (a) The photograph of the scaled-up synthesized solution indicating that PdNSs could be prepared on a large scale (500 mL or larger) owing to the mild synthetic condition (35 °C or room temperature) and simple composition of reaction solution. (b) The low-magnification TEM image of Pd nanosheets.

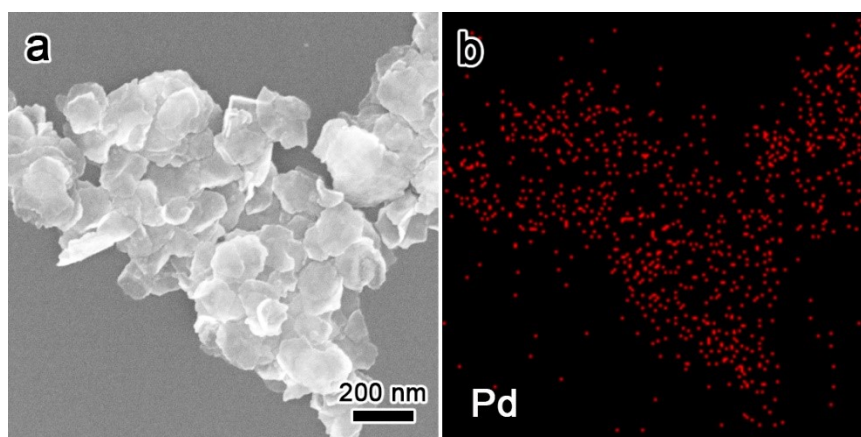


**Figure. S4.** (a) SEM image and the corresponding EDS mapping of PdNSs synthesized by using C22-pyB as the surfactants.

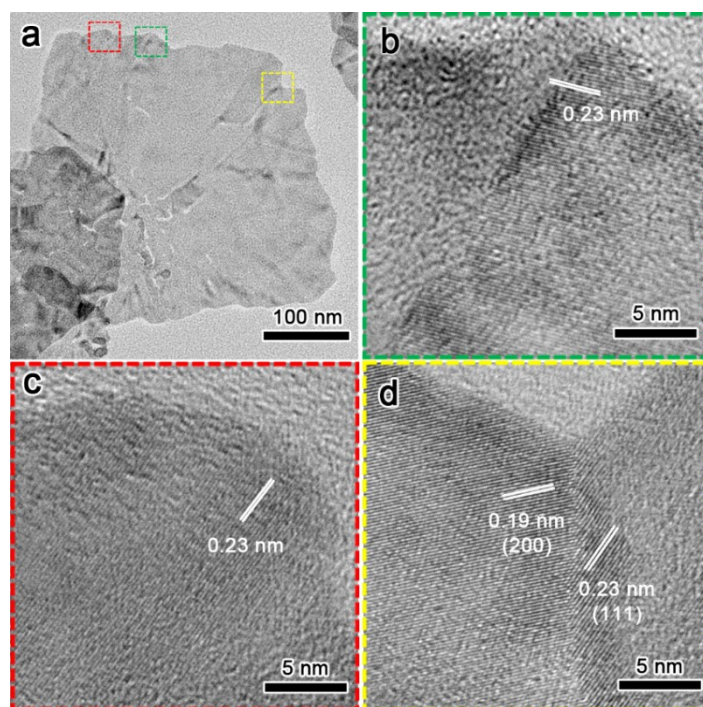


**Figure. S5.** (a) Low-magnification TEM image of an individual PdNS. (b-d) High-resolution TEM images taken from the different regions labeled by distinct colors in a. Except for the (111) planes, lattice fringes of  $\sim 0.19$  nm which can be indexed to (200) planes were also found. Both the presence of (111) and (200) planes indicates that the flat planes of PdNSs are covered by the  $\{111\}$  facets.

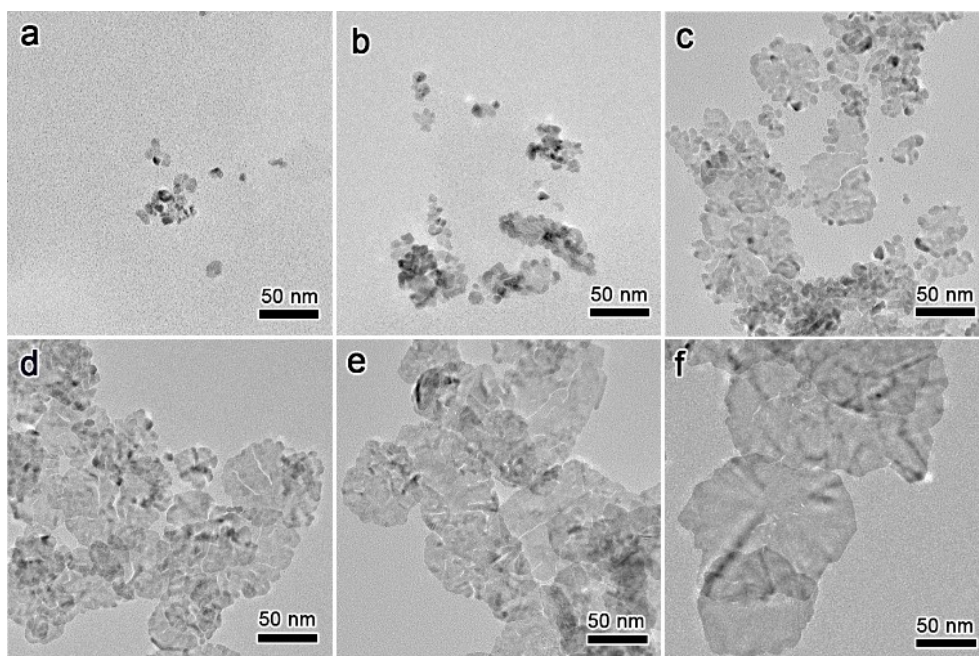


**Figure. S6** Representative TEM images of products captured at the different aging period by using C22-pyB as the surfactants.

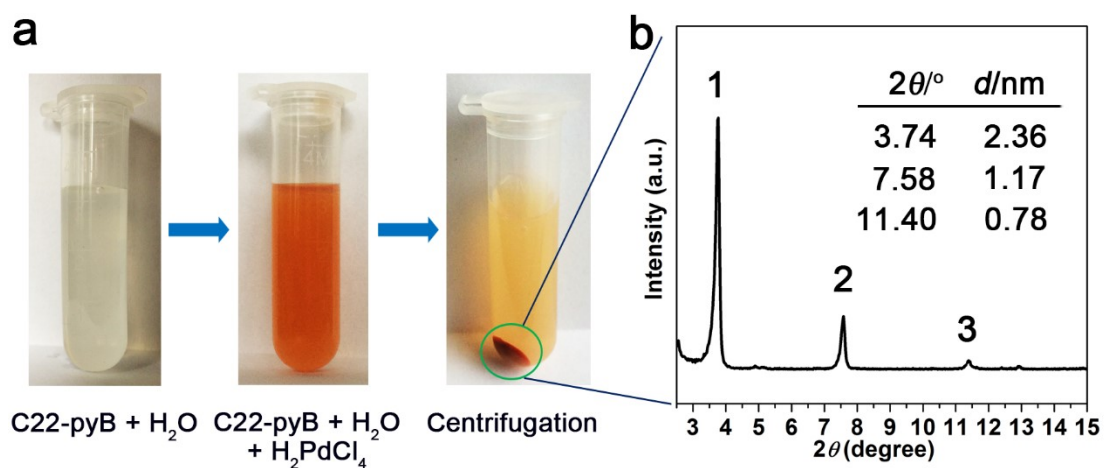


**Figure. S7.** (a) The hybrid inorganic-organic assemblies obtained by centrifugation of the mixture before the addition of AA. The reddish brown solids were slowly dried in a freeze dryer. (b) The small-angle XRD pattern of the powder indicating that the hybrid assemblies possess the lamellar mesostructure.

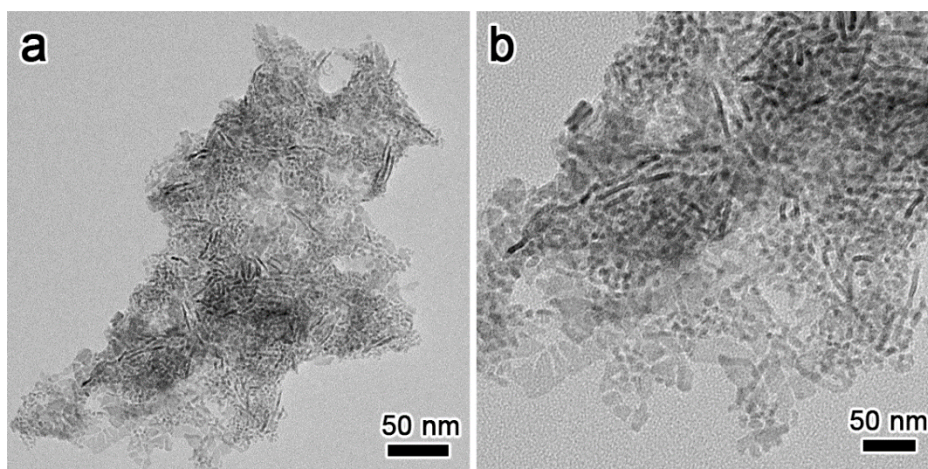


**Figure. S8.** TEM images of PdNSs synthesized by using hydrazine hydrate as the reduction agent. The ratio of the reactants keeps the same with the synthesis process by AA.

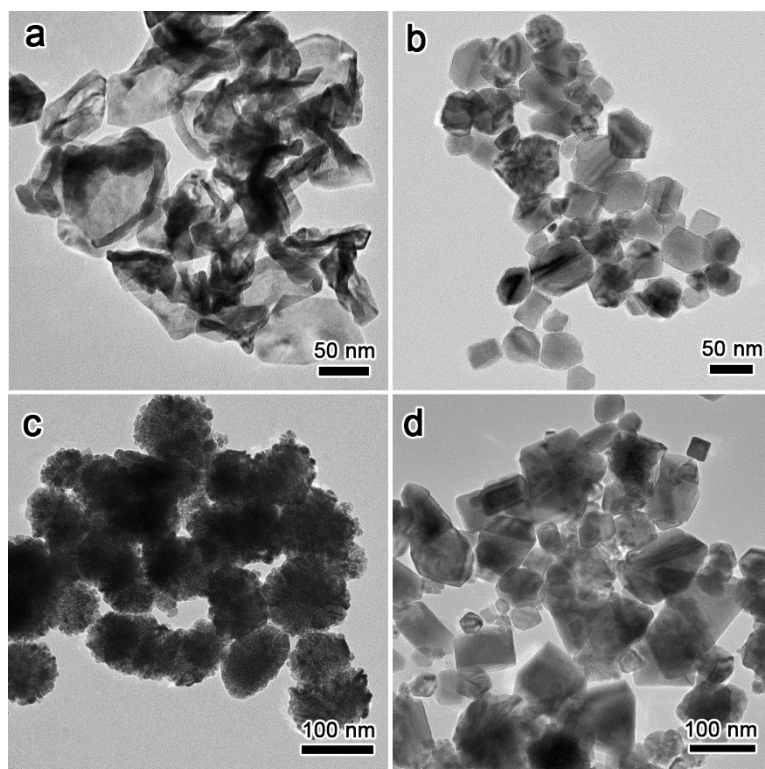


**Figure. S9.** Representative TEM images of Pd nanostructures synthesized by pyridinium-type surfactants with different carbon chains, (a) C20-pyB, (b) C18-pyB, (c) C16-pyB, (d) C14-pyB.

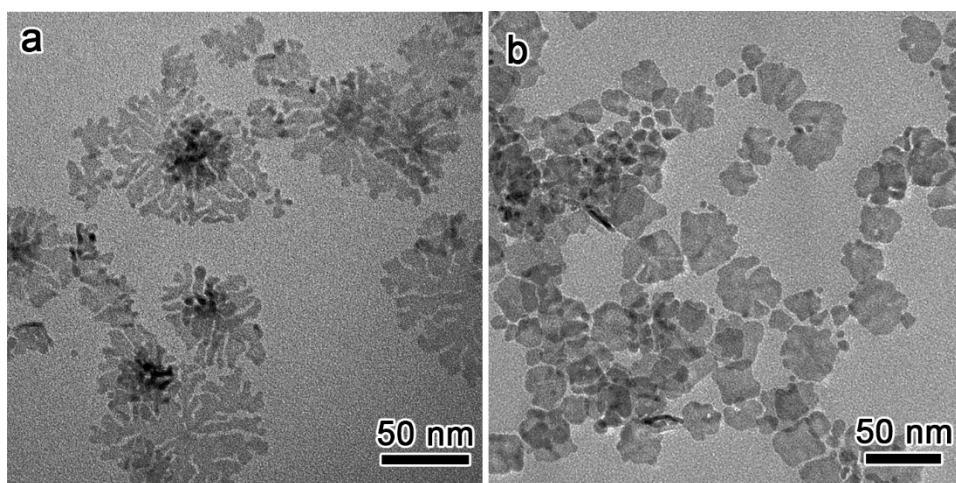


**Figure. S10.** TEM images of Pd nanosheets prepared by using surfactants C22-pyC (a) and C22-pyI (b) with the same synthesis conditions as C22-pyB. In the C22-pyI system, hydrazine hydrate, instead of AA, was employed as the reduction agent.

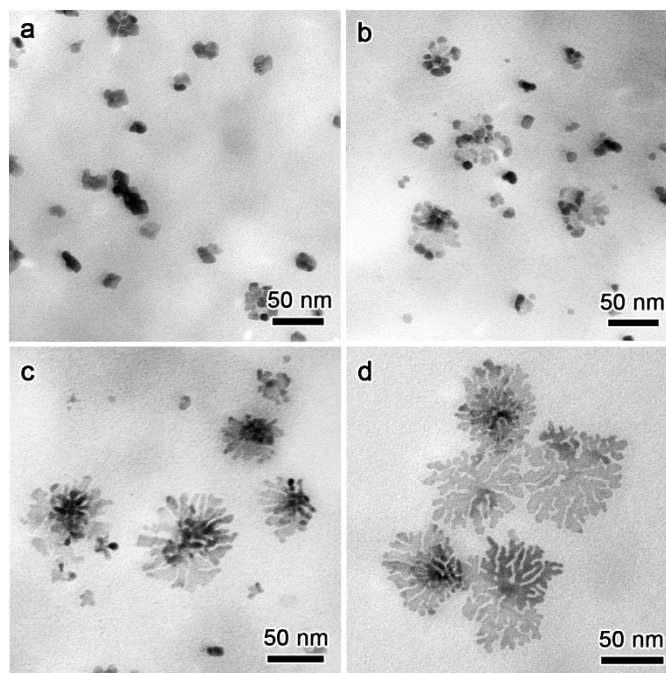


**Figure. S11.** Representative TEM images of Pd products obtained at different aging times by using C22-pyC as the surfactants, indicating the same nanosheets attachment growth process as the C22-pyB synthesis system.

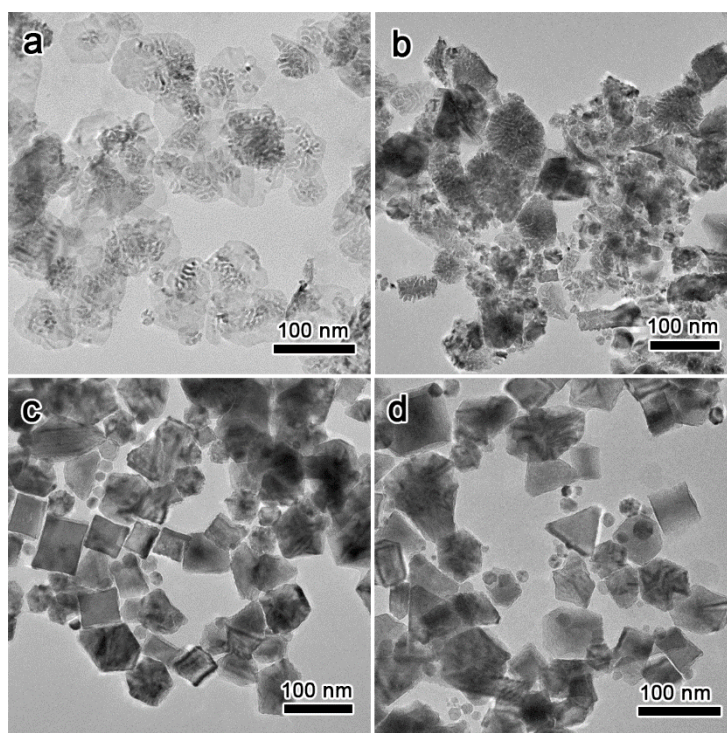


**Figure. S12.** TEM images of Pd nanostructures synthesized at different aging temperatures, 45 °C (a), 55 °C (b), 65 °C (c) and 85 °C (d).

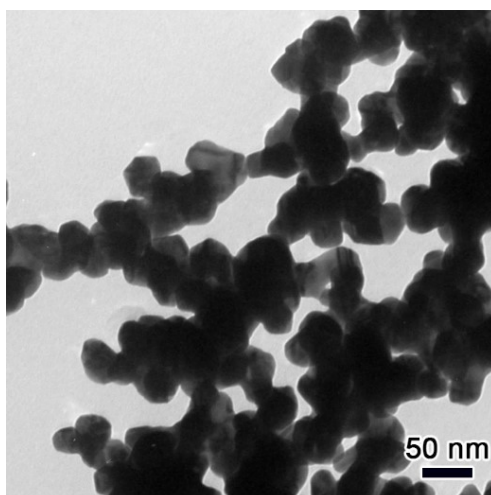


**Figure. S13.** TEM image of commercial palladium black used in the glycerol oxidation.

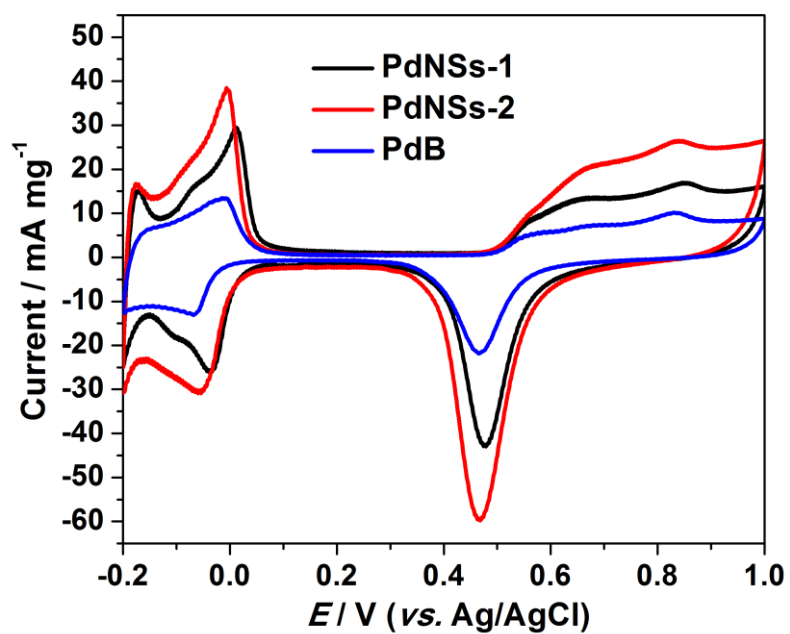


**Figure. S14.** CV curves of PdNSs-1, PdNSs-2 and PdB in 0.5 mol L<sup>-1</sup> H<sub>2</sub>SO<sub>4</sub> solution at a scan rate of 50 mV s<sup>-1</sup>.

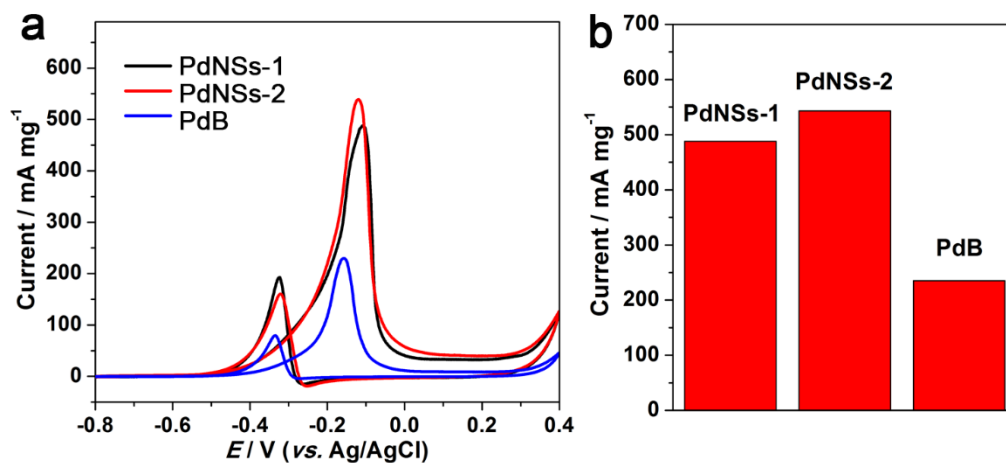


**Figure. S15.** (a) The metal mass-normalized CV curves of PdNSs-1, PdNSs-2 and PdB in 0.1 mol  $\text{L}^{-1}$  glycerol and 1 mol  $\text{L}^{-1}$  KOH. (b) Mass activity (via the forward peak current densities) of these Pd materials for glycerol electrooxidation.

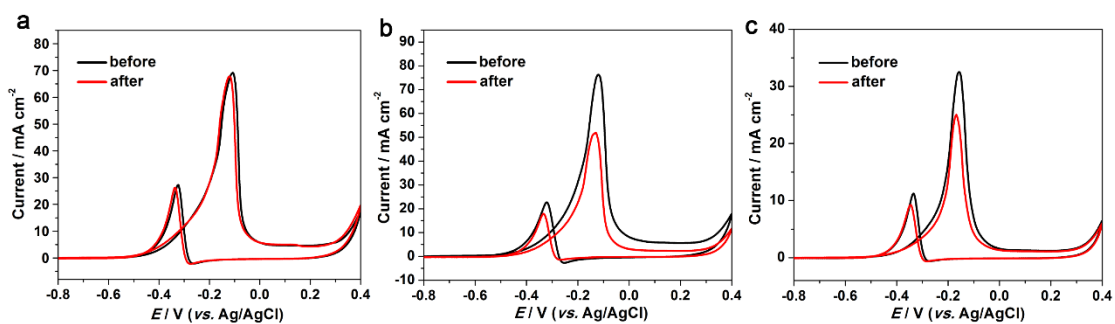


**Figure. S16.** CV curves of glycerol electrooxidation before and after the long-time current-time experiments on various Pd materials modified electrodes, PdNSs-1 (a), PdNSs-2 (b) and PdB (c).

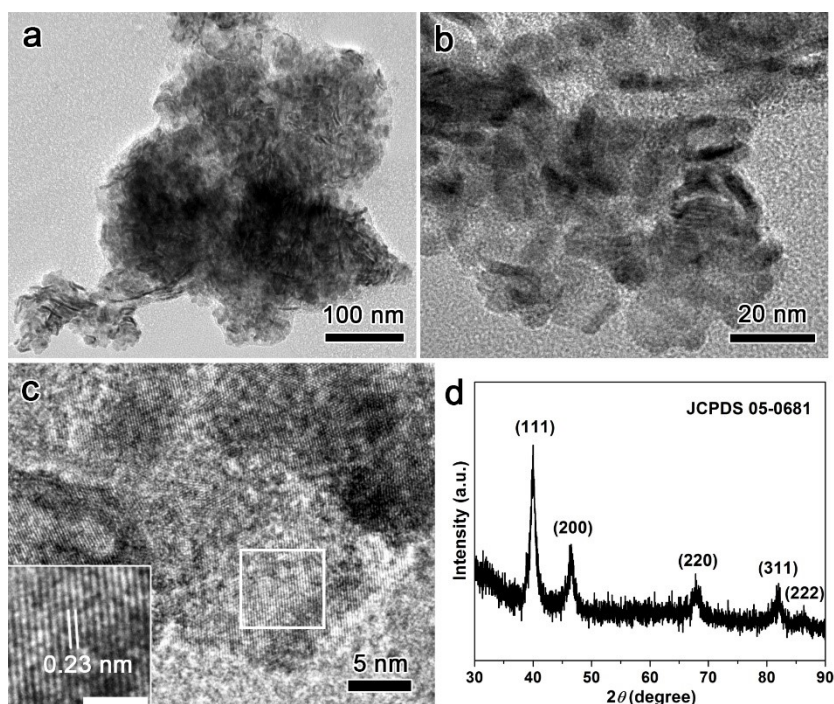


**Figure. S17.** (a-b) Low- and (c) high-resolution TEM images of PdNSs-2 after 8000 s stability test. (d) High-angle XRD pattern of PdNSs-2 after the stability test. The scale bar of insert in (c) is 2 nm. Compared to PdNSs-2 before the stability test, they could easily aggregate into bigger ones and the 2D ultrathin structure had been destroyed more or less after the stability test, which could result in a low electrocatalytic performance. However, the elemental Pd structure retained as suggested by the high-resolution TEM observation. The high-angle XRD pattern could further confirm the face-centered cubic Pd structure. The relatively weak peak intensity may be caused by the low Pd content (the final product contains a lot of Nafion).

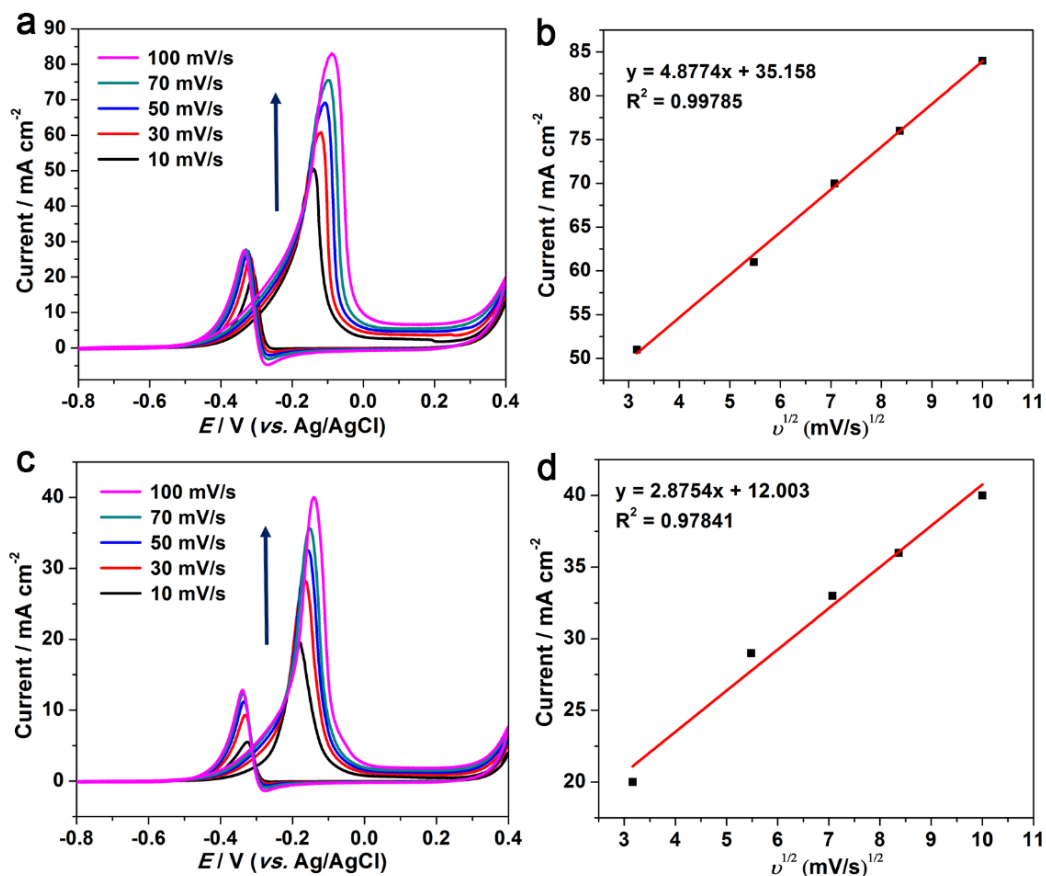


**Figure. S18.** CV curves of glycerol electrooxidation by PdNSs-1 at the different scan rates from 10 to 100  $\text{mV s}^{-1}$  (a) and the corresponding plot of  $j_p$  versus  $v^{1/2}$  (b). CV curves of glycerol electrooxidation by PdB at the different scan rates (c) and the corresponding plot of  $j_p$  versus  $v^{1/2}$  (d).

**Table S1.** The concentration of different reactants for the synthesis of PdNSs with distinct diameters.

| Average diameters<br>of PdNSs | The amount of different reactants <sup>a</sup> |   |           |                      |
|-------------------------------|--|---|-----------|----------------------|
|                               | C22-pyB (mmol)                                 | H <sub>2</sub> PdCl <sub>4</sub> (mmol) | AA (mmol) | H <sub>2</sub> O (g) |
| 20 nm                         | 0.05   | $4 \times 10^{-3}$                      | 0.3       | 10                   |
| 50 nm                         | 0.1  | $4 \times 10^{-3}$                      | 0.3       | 10                   |
| 100 nm                        | 0.2  | $8 \times 10^{-3}$                      | 0.3       | 10                   |
| 200 nm                        | 0.2  | $3 \times 10^{-2}$                      | 0.6       | 10                   |

<sup>a</sup> All of the aging temperature in these synthesis cases is set to 35 °C.

## Reference

[1] Biegler T, Rand D A J, Woods R. *J. Electroanal. Chem.*, 1971, 29(2): 269-277.